Alternative Size and Lifetime Measurements for High-Energy Heavy-Ion Collisions

Scott Pratt and Silvio Petriconi

Department of Physics and Astronomy, Michigan State University, East Lansing Michigan, 48824

(Dated: August 28, 2003)

Two-Particle correlations based on the interference of identical particles have provided the chief means for determining the shape and lifetime of sources in relativistic heavy ion collisions. Here, Strong and Coulomb induced correlations are shown to provide similar information.

In the collision of highly relativistic heavy ions, an excited region of matter is created where novel states of matter are expected to be exist. These transient states, which occupy thousands of fm^3, are expected to dissolve on a time scale of 10 fm/c. Only the momenta of the collision debris are experimentally accessible. However, space-time information is crucial for understanding the reaction [1]. Most importantly, a latent heat associated with a phase transition would be accompanied by a significant enhancement to the duration of the emitting phase[2–5]. The most direct means for determining the spatial and temporal characteristics of the reaction is through the experimental measure of the two-particle correlation function which describes the ratio of the two-particle probability to the product of the single-particle probabilities for emitting species a and b with momenta p_a and p_b.

The correlation of two particles with outgoing momenta, p_a and p_b, is determined by $g(\mathbf{v}, \mathbf{r})$, the normalized probability of two particles being emitted with the same velocity $\mathbf{v}$, and being separated by a distance $\mathbf{r}$, as measured in the two-particle center-of-mass frame.

$$C(\mathbf{v}, \mathbf{q}) = \int d^3 r \, g(\mathbf{v}, \mathbf{r}) |\psi(\mathbf{q}, \mathbf{r})|^2. \tag{1}$$

Here, $\mathbf{q} = \mathbf{p}'_a = -\mathbf{p}'_b$ is the relative momentum in the center-of mass frame and $\mathbf{v}$ is the velocity of the pair's center of mass. If the particles are distinguishable and do not interact with one another, the wave function, $\psi(\mathbf{q}, \mathbf{r})$, would be $e^{i\mathbf{q}\cdot\mathbf{r}}$, and the resulting correlation would be unity. Since the correlation function can be analyzed for any total momentum and for any choice of species a and b, a wealth of information regarding the space-time characteristics of the source is available.

A measurement of $C(\mathbf{v}, \mathbf{q})$ represents three dimensions of information for particles of a given velocity $\mathbf{v}$, and can, at best, lead to a unique extraction of $g(\mathbf{v}, \mathbf{r})$. Unfortunately, complete knowledge of $g(\mathbf{v}, \mathbf{r})$ does not uniquely provide all spatial and temporal information about the source which would require four dimensions of information for each velocity. Nonetheless, one can infer the emission time scale if the source is long lived. To demonstrate this, we consider a Gaussian source characterized by a transverse spatial size $R_\perp$ and a lifetime τ. The source is defined in a frame moving along the beam axis such that the longitudinal (along the beam axis) component of the pair's momentum is zero, i.e., the velocity $\mathbf{v}$ is perpendicular to the beam. This is referred to as the longitudinally co-moving frame, which we delineate with primes.

$$\begin{aligned} S(\mathbf{v}, x') &= \frac{dN}{d^4 x \, d^3 v} \\ &\propto \exp\left\{ \frac{-x'^2_{\text{out}}}{2R_\perp^2} - \frac{-x'^2_{\text{side}}}{2R_\perp^2} - \frac{-x'^2_{\text{long}}}{2R_{\text{long}}^2} - \frac{-x'^2_0}{2\tau^2} \right\}. \end{aligned} \tag{2}$$

Consistent with the usual convention used in the field, the three dimensions are referred to as the longitudinal (along the beam axis), outwards (parallel to $\mathbf{v}$) and the sidewards direction (perpendicular to both the beam axis and $\mathbf{v}$). The correlation function depends only on $g(\mathbf{v}, \mathbf{r})$, the distribution of relative coordinates of particles moving with the same velocity.

$$g(\mathbf{v}, \mathbf{r}) = \int d^4 x_a d^4 x_b \, S_a(\mathbf{v}, x_a) S_b(\mathbf{v}, x_b) \delta^3(\mathbf{x}_a - \mathbf{x}_b - \mathbf{r}), \tag{3}$$

where $\mathbf{r}$, $\mathbf{x}_a$ and $\mathbf{x}_b$ are all measured in the rest frame of the pair. For the Gaussian source described above, this results in

$$g(\mathbf{v}, \mathbf{r}) \propto \exp\left\{ \frac{-r^2_{\text{out}}}{4\gamma_v^2(R_\perp^2 + v^2\tau^2)} - \frac{-r^2_{\text{side}}}{4R_\perp^2} - \frac{-r^2_{\text{long}}}{4R_{\text{long}}^2}, \right\}$$

$$R_{\text{side}} = R_\perp, \quad R_{\text{out}} = \gamma_v\sqrt{R_\perp^2 + v^2\tau^2}. \tag{4}$$

Given the fact that τ can depend on the velocity, one can not determine τ directly, but must instead extract R_{side} and R_{out} from a direct fit to experimental correlation functions, then rely on the assumption that any difference between R_{out} and R_{side} (aside from that due to the Lorentz contraction factor) is the result of a non-zero lifetime. This assumption becomes questionable when the lifetimes are short. In the convention above, which will be used throughout the paper, R_{out} refers to the size measured by an observer moving with the pair. This differs from standard practice where R_{out} usually refers to the size measured by an observer in the longitudinally co-moving frame, which is shorter by a factor $1/\gamma_v$ due to Lorentz contraction.

Dynamical models that incorporate a phase transition with a latent heat predict longer emission times than

models with no latent heat [2–5]. These models predict continuous emission over times which can be in excess of 20 fm/c. Remarkably, analyses of two-pion interferometry at RHIC show equal outwards and sidewards sizes when viewed in the longitudinally co-moving frame, i.e., $R_{\text{out}}/\gamma_v \sim R_{\text{side}}$ [7–9]. This suggests that the emission is sudden rather than continuous. Furthermore, the experimental values of R_{long} are shorter than what was expected from the dynamical models, suggesting that the time of this sudden disintegration is relatively short, ~ 10 fm/c after the beginning of the collision. The two-pion analyses are based on the interference associated with symmetrizing same-sign pions. As the existence or non-existence of a latent heat with the QCD deconfinement transition represents a central issues of the RHIC program, it is imperative to explore alternative means for measuring the size and shape of the emission sources.

For non-interacting identical particles the wave function has a simple form,

$$|\psi(\mathbf{q}, \mathbf{r})|^2 = 1 \pm \cos(2\mathbf{q} \cdot \mathbf{r}). \tag{5}$$

By performing an inverse Fourier transform of $C(\mathbf{v}, \mathbf{q}) - 1$ in Eq. (1), one can obtain $g(\mathbf{v}, \mathbf{r})$. Even though the pions are charged, experimental analyses have tried to ignore the Coulomb interaction as much as possible, and in fact try to "correct" their data as to best eliminate the effects of Coulomb from the correlation function so that comparison with simple forms for $g(\mathbf{v}, \mathbf{r})$ is easily accommodated. The aim of this paper is to demonstrate that Coulomb and strong interactions between the pair should not only be included in correlation analyses, but that they provide tremendous leverage for determining both the size and shape of $g(\mathbf{v}, \mathbf{r})$.

First, we consider two particles which interact only via the Coulomb interaction. Correlations for pK^+ from a Gaussian source,

$$g(\mathbf{v}, \mathbf{r}) = \frac{1}{(4\pi)^{3/2} R_{\text{out}} R_\perp^2} \exp\left\{ -\frac{r_{\text{out}}^2}{4R_{\text{out}}^2} - \frac{r_{\text{side}}^2 + r_{\text{long}}^2}{4R_\perp^2} \right\}, \tag{6}$$

are displayed in Fig. 1 as a function of $Q_{\text{inv}} = 2q = \sqrt{-(p_a - p_b)^2 + (m_a^2 - m_b^2)^2/P^2}$. The source sizes are chosen $R_{\text{out}} = 8$ fm and $R_\perp = 4$ fm. The integration described in Eq. (1) was performed with Monte Carlo methods. The Coulomb plane waves are solution to Schrödinger's equation for a wave where the outgoing wave has momentum $\mathbf{q}$.

$$-\nabla^2 \psi(\mathbf{q}, \mathbf{r}) + q \frac{2\eta}{r} \psi(\mathbf{q}, \mathbf{r}) = q^2 \psi(\mathbf{q}, \mathbf{r}), \tag{7}$$

where η is the Sommerfeld parameter,

$$\eta = \frac{Z_a Z_b \mu e^2}{q}, \quad \mu = \frac{E_a' E_b'}{(E_a' + E_b')}. \tag{8}$$

The usual definition of the reduced mass μ, involving m_a and m_b, has been altered to achieve consistency with relativistic treatments for small e^2.
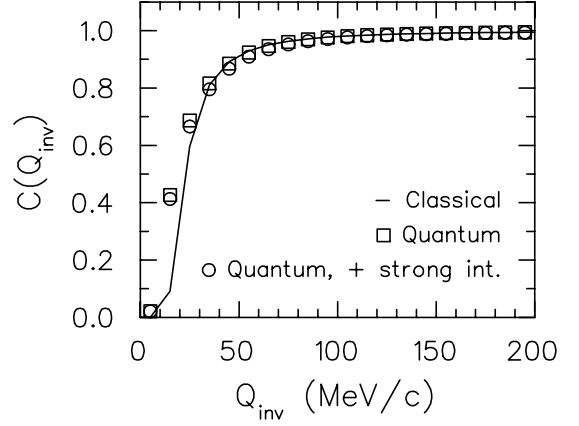

FIG. 1: pK^+ correlations are shown for a Gaussian source ($R_{\text{long}} = R_{\text{side}} = 4$ fm, $R_{\text{out}} = 8$ fm). The classical approximation well explains Coulomb correlations at large relative momentum. The strong interaction only moderately affects the correlation function.

In order to understand the form of the squared wave function, it it insightful to compare to the classical approximation where the squared wave function in Eq. (1) is replaced by the ratio of the initial and final phase space [10].

$$|\psi(\mathbf{q}, \mathbf{r})|^2 \rightarrow \frac{d^3 q_0}{d^3 q} = \frac{1 + \cos\theta_{qr} - \eta/(qr)}{\sqrt{(1 + \cos\theta_{qr})^2 - 2(1 + \cos\theta_{qr})\eta/(qr)}} \\ \cdot \Theta(1 + \cos\theta_{qr} - 2\eta/(qr)), \tag{9}$$

where θ_{qr} is the angle between $\mathbf{q}$ and $\mathbf{r}$. Integrating over $\cos\theta_{qr}$, one finds the angle-averaged correlation weight,

$$\frac{q_0^2 dq_0}{q^2 dq} = \sqrt{1 - \frac{2\eta}{qr}} \approx 1 - \frac{\eta}{qr}. \tag{10}$$

In the non-relativistic limit $\eta \propto 1/q$ and $C(q)$ approaches unity as $1/q^2$. Thus, the tail of the correlation function provides a measure of the expectation, $\langle 1/r \rangle$.

Convoluting the phase-space focusing factor in Eq. (9) with the Gaussian source function gives a classical result for the correlation function,

$$C_{\text{classical}}(\mathbf{q}) = \int d^3 r \frac{1}{(4\pi)^{3/2} R_{\text{out}} R_{\text{side}} R_{\text{long}}}$$
$$\cdot \exp\left(-\frac{r_{\text{out}}^2}{4R_{\text{out}}^2} - \frac{r_{\text{side}}^2}{4R_{\text{side}}^2} - \frac{r_{\text{long}}^2}{4R_{\text{long}}^2} \right)$$
$$\cdot \frac{1 + \cos\theta_{qr} - \eta/(qr)}{\sqrt{(1 + \cos\theta_{qr})^2 - 2(1 + \cos\theta_{qr})\eta/(qr)}}$$
$$\cdot \Theta(1 + \cos\theta_{qr} - 2\eta/(qr)).$$

Performing the integral with Monte-Carlo techniques is non-trivial due to the non-analytic behavior of $d^3 q_0 / d^3 q$ which has an integrable singularity. The singularity can

be overcome by choosing the direction of $\mathbf{q}$ as the polar axis in spherical coordinates, then making a variable substitution,

$$u = \sqrt{(1 + \cos\theta_{qr} - \gamma)^2 - \gamma^2}, \qquad (11)$$
$$\gamma \equiv \eta/(qr).$$

The integral can then be expressed in terms of u,

$$C_{\text{classical}}(\mathbf{q}) = \int_0^{2\pi} d\phi \int_0^{2\sqrt{1-\gamma}} du \int r^2 dr \qquad (12)$$
$$\cdot \frac{1}{(4\pi)^{3/2} R_{\text{max}}^3} \exp\left(-\frac{r^2}{4R_{\text{max}}^2}\right) \frac{1}{\sqrt{1-\gamma}} w(r, u, \phi),$$

$$w(r, u, \phi) = \frac{R_{\text{max}}^3}{R_{\text{out}} R_{\text{side}} R_{\text{long}}} \Theta(1-\gamma)\sqrt{1-\gamma} \qquad (13)$$
$$\cdot \exp\left(\frac{r^2}{4R_{\text{max}}^2} - \frac{r_{\text{out}}^2}{4R_{\text{out}}^2} - \frac{r_{\text{side}}^2}{4R_{\text{side}}^2} - \frac{r_{\text{long}}^2}{4R_{\text{long}}^2}\right).$$

Monte Carlo methods can then be used to calculate the integral as $C_{\text{classical}} = \langle w \rangle$, when u is sampled uniformly and r is sampled according to a Gaussian distribution governed by R_{max}, which is the largest of the three dimensions.

The classical and quantum results are remarkably similar for large q as can be seen in Fig. 1. Extracting the shape of the source requires measuring $C(\mathbf{v}, \mathbf{q})$ as a function of the direction of $\mathbf{q}$. Since the correlation approaches unity as $1/q^2$, we recommended plotting $q^2[C(q) - 1]$ rather than $C(q)$ so that the main q dependence can be ignored, allowing the use of larger bins in q.

As a function of the direction of $\mathbf{q}$, correlations are shown in Fig. 2 for $Q_{\text{inv}} = 30$ and 150 MeV/c alongside analogous results calculated with the classical form described in Eq. (9). The negative correlation at $\cos\theta = \pm 1$ derives from the fact that the relative momentum of the two positive particles are deflected away from the direction defined by their relative position by the repulsive Coulomb force. Careful analysis of the classical expression, Eq. (9), shows that for small η, the negative correlation is confined to angles where $\mathbf{q}$ and $\mathbf{r}$ are anti-parallel. Since this angular range is small, the angular dependence can be approximated by a delta function that integrates to the same net strength.

$$\frac{d^3 q_0}{d^3 q} \approx 1 - (2\eta/qr)\delta(1 + \cos\theta_{qr}). \qquad (14)$$

For an elliptical source, the fraction of the ellipse's volume confined to a small cone of solid angle $\Delta\Omega$ along the direction of R_{out} is $\Delta\Omega R_{\text{out}}^3/(R_{\text{out}} R_{\text{side}} R_{\text{long}})$. The prefactor, (η/qr), in Eq. (14) also contributes a factor of $1/R_{\text{out}}$, so the net strength of the correlation function for $\mathbf{q}$ pointing in the outwards direction scales as $R_{\text{out}}^2/(R_{\text{out}} R_{\text{side}} R_{\text{long}})$. This means that the correlation
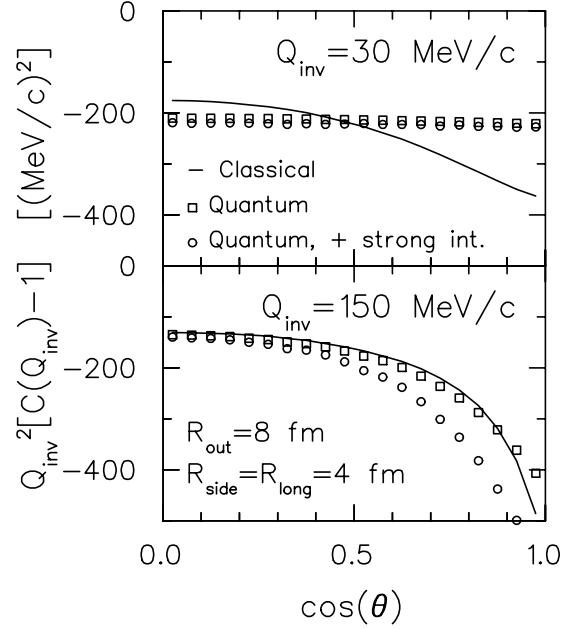

FIG. 2: pK^+ correlations are shown as a function of the angle of the relative momentum relative to the outwards direction for the Gaussian source ($R_{\text{long}} = R_{\text{side}} = 4$ fm, $R_{\text{out}} = 8$ fm). The classical approximation becomes reasonable for large Q_{inv} where the ratio of the suppression at $\cos\theta = 1$ to the suppression at $\cos\theta = 0$ approaches $(R_{\text{out}}/R_{\text{side}})^2$.

is stronger in the outward direction than in the sideward direction by a factor of $R_{\text{out}}^2/R_{\text{side}}^2$. Thus, the negative correlation in Fig. 2 is four times deeper for $\cos\theta = 1$ than it is for $\cos\theta = 0$ for the classical calculation. The same calculation with $R_{\text{out}}/R_{\text{side}} = 3$ indeed resulted in a correlation that was nine times deeper for $\cos\theta = 1$. Since the θ dependence in the correlation behaves as the square of the asymmetry, these measurements provide an excellent means to extract all three dimensions of the source. This allows one to infer both the duration of the emission from the $R_{\text{out}}/R_{\text{side}}$ ratio and the time of the emission for the R_{long} measurement. The sensitivity to the asymmetry in the quantum calculations was only slightly muted relative to the classical calculations for $Q_{\text{inv}} > 100$ MeV/c.

It should not be particularly difficult to obtain the required statistics even though the correlation is of the order of 1%. Although the correlation falls as $1/Q_{\text{inv}}^2$, phase space rises as Q_{inv}^2. Unlike identical-particle correlations at small relative momentum, there are no issues with two-track resolution. However, one has to consider large-scale correlations, e.g., collective flow, jets and charge conservation. Correlation from charge conservation can be neglected by considering only same-sign pairs. Collective flow can be eliminated by carefully constructing the correlation denominator with pairs from events with the same reaction plane. Such competing correlations ultimately limit the range in Q_{inv} that is useful for the

analysis. For instance, if the uncertainty of the competing correlations for pK^+ is of the order of 1%, the analysis should be restricted to $Q_{inv} < 150$ MeV/c so that Coulomb remains the dominant factor.

The angular sensitivity of Coulomb-induced correlations have been investigated in intermediate-energy heavy-ion collisions. These studies involved light fragments, e.g. Carbon-Carbon, which can be treated with classical trajectories [10]. The Coulomb mean field from the remainder of the source was found to distort the the shape information. However, the residual Coulomb interaction is expected to play a much smaller role at RHIC where the hadrons move much faster and spend less time interacting with the mean field. Furthermore, analyses can be performed with both positive and negative pairs, e.g., both pK^+ and $\bar{p}K^-$. Averaging the two correlation functions should largely cancel the effects of the residual interaction.

The angular dependence of Coulomb correlations of non-identical particles have been used to determine the degree to which one species is displaced relative to another [11–15]. These studies involved comparing correlations for $\cos\theta < 0$ with correlations with $\cos\theta > 0$. This comparison effectively provides a measure of the dipole moment of the the source function, whereas the comparison of the correlation function for $\cos\theta = 0$ and $\cos\theta = \pm 1$ is sensitive to the quadrupole moment, i.e., R_{out}/R_{side}.

Finally, we make some comments concerning the validity of using classical rather than quantum formalism to calculate correlations. The validity of classical forms depends on the source size, the value of the relative momentum, and the charges and masses of the particles. For a source of characteristic size R, classical forms work well whenever $qR >> 1$. For source sizes at RHIC, this implies that classical calculations should begin to be valid for Q_{inv} greater than 100 MeV/c, which is indeed seen in Fig.s 1 and 2. Unfortunately, this range of validity is outside the low q region where most of the investigations into two-particle correlations have been focused. The momentum scale of the Coulomb hole is determined by the classical turning point, $q^2/(2\mu) = e^2/R$. If one adds the constraint $qR \geq 1$, one finds that classical considerations would be valid deep into the Coulomb hole if $R > 1/(2me^2)$, or one half the Bohr radius. Since the two pion Bohr radius, 387 fm, is much larger than characteristic sources sizes, classical considerations are applicable only in the tail of the correlation function for hadron-hadron correlations. In reference [16] classical ideas were applied for hadron-hadron correlations. As can be seen from the comparison of quantum results and classical results for the angular correlations in Fig. 2, classical models should not be applied except at high q. Our motivation in performing classical calculations derives from the fact that they are more physically intuitive and analytically simpler. They provide insight into how the angular correlations are related to the size and spatial anisotropy of the source. As the quantum calculations are not challenging numerically, there is little reason to forgo the full quantum treatments.

Incorporating the strong interaction into the wave function in Eq. (1) is straight-forward if the the strong interaction can be expressed as a non-relativistic potential. One must simply solve the Schrödinger equation. However, many interactions can not be expressed in terms of such potentials. For instance, the interaction of a π^+ and proton through the delta resonance involves a quantum rearrangement of the participating quarks. Thus, a wave function is not a meaningful quantity for separations below $\epsilon \sim 1$ fm, but it is certainly a well defined object for $r > \epsilon$, and can be expressed in terms of a Coulomb wave with the incoming partial waves are modified by phase shifts.

$$
\begin{aligned}
\psi(\mathbf{q}, \mathbf{r}) = \psi_0(\mathbf{q}, \mathbf{r}) + \sum_\ell \sqrt{4\pi(2\ell+1)}\frac{i^\ell}{2qr}e^{-i\sigma_\ell} \\
\cdot (F_\ell(\eta, qr) - iG_\ell(\eta, qr))\left(e^{-2i\delta_\ell} - 1\right)Y_{\ell, m=0}, \\
\sigma_\ell \equiv \arg\left(\Gamma(1 + \ell + i\eta)\right).
\end{aligned}
\tag{15}
$$

Here, F_ℓ and G_ℓ are the regular and irregular partial Coulomb waves and the second term describes the distortion of the incoming partial wave, $F_\ell - iG_\ell$.

For the $p\pi^+$ and pK^+ examples discussed in this study, the plane wave also has a spin index, $m_s = \pm 1/2$, which is not conserved for partial waves with $\ell > 0$. The states of a given m_s must be decomposed in terms of eigenstates of total angular momentum which are phase shifted by eigen-phases, $\delta_{\ell,j}$. After applying angular momentum algebra, Eq. (15) can be modified to include flipping the spin. For $\ell = 1$,

$$
(e^{-2i\delta_{\ell=1}} - 1)Y_{\ell=1, m=0} \rightarrow
$$

$$
e^{-2i\delta_{\ell=1, j=3/2}}\sqrt{\frac{2}{3}}|j=3/2, m_j=1/2\rangle
$$

$$
+ e^{-2i\delta_{\ell=1, j=1/2}}\sqrt{\frac{1}{3}}|j=1/2, m_j=1/2\rangle - Y_{\ell=1, m=0}|\uparrow\rangle
$$

$$
= e^{-2i\delta_{\ell=1, j=3/2}}\left(\frac{2}{3}Y_{\ell=1, m=0}|\uparrow\rangle + \frac{\sqrt{2}}{3}Y_{\ell=1, m=1}|\downarrow\rangle\right)
$$

$$
+ e^{-2i\delta_{\ell=1, j=1/2}}\left(\frac{1}{3}Y_{\ell=1, m=0}|\uparrow\rangle - \frac{\sqrt{2}}{3}Y_{\ell=1, m=1}|\downarrow\rangle\right)
$$

$$
- Y_{\ell=1, m=0}|\uparrow\rangle
$$

$$
= \left(\frac{2}{3}e^{-2i\delta_{\ell=1, j=3/2}} + \frac{1}{3}e^{-2i\delta_{\ell=1, j=1/2}} - 1\right)Y_{\ell=1, m=0}|\uparrow\rangle
$$

$$
+ \frac{\sqrt{2}}{3}\left(e^{-2i\delta_{\ell=1, j=3/2}} - e^{-2i\delta_{\ell=1, j=1/2}}\right)Y_{\ell=1, m=1}|\downarrow\rangle.
\tag{16}
$$

Only the first term interferes with the original partial wave when calculating $|\psi(\mathbf{q}, \mathbf{r})|^2$. In principle, the dis-

torted incoming wave can be calculated from the eigen-phases if one knows the basis, e.g., total angular momentum for this case. In this example the sum of the intrinsic spins was 1/2. For higher spins, one would have to consider the mixing of different orbital angular momenta, e.g., the mixing of the $\ell = 0$ and $\ell = 2$ states for proton neutron interactions. For such problems, one must know the mixing factors in addition to the eigen-phases. Thus, if one understands the S-matrix elements in the partial wave basis, one can always construct the $\psi(\mathbf{q}, \mathbf{r})$ for r greater than the interaction range.

For $r < \epsilon$, one must use an effective form for $|\psi(\mathbf{q}, \mathbf{r})|^2$. Since ϵ is much smaller than any characteristic dimension of the source, only the integral of ψ^2 matters in the region less than ϵ, and one can safely choose,

$$|\psi(\mathbf{q}, r < \epsilon)|^2 = |\psi_0(\mathbf{q}, \mathbf{r})|^2 + W(\epsilon, q), \qquad (17)$$

where ψ_0 is the Coulomb wave and W is independent of r. The change in the density of states can be expressed both in terms of phase shifts and wave functions [17],

$$
\begin{aligned}
\Delta \frac{dN}{dq} &= \frac{4\pi q^2}{(2\pi)^3} \int d^3 r \left(|\psi(\mathbf{q}, \mathbf{r})|^2 - |\psi_0(\mathbf{q}, \mathbf{r})|^2 \right) \qquad (18) \\
&= \sum_\ell \frac{(2\ell + 1)}{\pi} \frac{d\delta_\ell}{dq} \\
&= \frac{2q^2 \epsilon^3}{3\pi} W(\epsilon, q) \\
&+ 2 \sum_\ell \frac{(2\ell + 1)}{\pi} \int_\epsilon^\infty dr \left(|\phi_\ell(\eta, qr)|^2 - |F_\ell(\eta, qr)|^2 \right), \\
\phi_\ell &= F_\ell + \frac{1}{2}(e^{-2i\delta_\ell} - 1)(F_\ell - iG_\ell).
\end{aligned}
$$

Thus, W can be expressed in terms of derivatives of the phase shifts and integrals of the type,

$$I_\ell(\epsilon, q, \delta_\ell) \equiv \int_\epsilon^\infty dr |\phi_\ell(\eta, qr, \delta_\ell)|^2, \qquad (19)$$

Since ϕ_ℓ is a solution to the Schrödinger equation, one can rewrite I_ℓ, assuming that ϕ and ϕ' are solutions with energy eigenvalues $q^2/2\mu$ and $q'^2/2\mu$ with $q \sim q'$,

$$
\begin{aligned}
(q'^2 - q^2) I_\ell(\epsilon, q, \delta_\ell) &= \Re \int_\epsilon^\infty dr \left(\partial_r^2 \phi_\ell'^* \phi_\ell - \phi_\ell'^* \partial_r^2 \phi_\ell \right) \\
I_\ell(\epsilon, q, \delta_\ell) &= -\frac{1}{2q} \Re \left(\partial_r \phi_\ell^* \partial_q \phi_\ell - \phi_\ell^* \partial_r \partial_q \phi_\ell \right) \Big|_\epsilon^\infty.
\end{aligned}
\qquad (20)
$$

Transforming the derivatives to the variables η and $x = qr$ facilitates use of the recursion relations for the
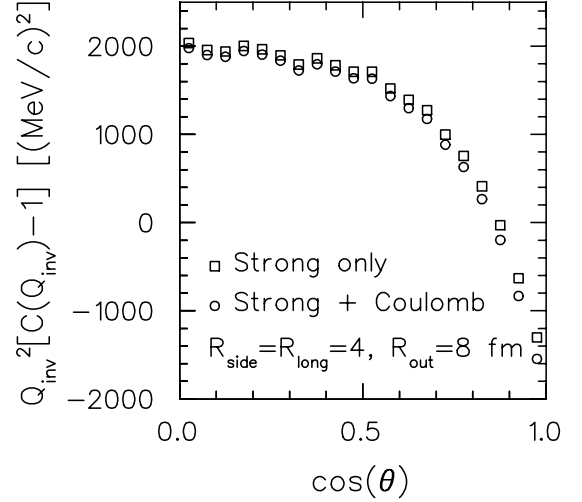

FIG. 3: $p\pi^+$ angular correlations for a Gaussian source ($R_{\text{out}} = R_{\text{side}} = 4$ fm, $R_{\text{long}} = 8$ fm) with $Q_{\text{inv}} = 450$ MeV/c. At this Q_{inv} the correlation is dominated by the Δ^{++} resonance. The behavior at $\cos\theta = 1$ is due to interference between the scattered partial wave and the initial plane wave.

Coulomb wave functions [18],

$$
\begin{aligned}
I_{\ell \neq 0}(\epsilon, q, \delta_\ell) =& \left(\phi_\ell^* \phi_\ell + \phi_{\ell-1}^* \phi_{\ell-1} \right) \frac{x}{2q\ell^2} (\ell^2 + \eta^2) \\
& - \Re(\phi_{\ell-1}^* \phi_\ell) \frac{(2\ell+1)(\ell^2 + \eta^2)\ell + 2\eta x(\ell^2 + \eta^2) + \ell \eta^2}{2q\ell^2 \sqrt{\ell^2 + \eta^2}} \\
& + \Re\left(\phi_\ell \partial_\eta \phi_{\ell-1}^* - \phi_{\ell-1} \partial_\eta \phi_\ell \right) \frac{\eta \sqrt{\ell^2 + \eta^2}}{2q\ell} \Bigg|_{x=q\epsilon}, \\
I_{\ell=0}(\epsilon, q, \delta_\ell) =& (\phi_0^* \phi_0 + \phi_1^* \phi_1) \frac{x(1 + \eta^2)}{2q} \\
& - \Re(\phi_0^* \phi_1) \frac{(1 + \eta^2)(1 + 2\eta x) + \eta^2}{2q\sqrt{1 + \eta^2}} \\
& + \Re(\phi_1^* \partial_\eta \phi_0 - \phi_0^* \partial_\eta \phi_1) \eta \frac{\sqrt{1 + \eta^2}}{2q} \Bigg|_{x=q\epsilon}.
\end{aligned}
\qquad (21)
$$

The upper limit, $x = \infty$, need not be evaluated since it would be canceled by an equal and opposite contribution from the non-phaseshifted term in Eq. (18). For the case with no Coulomb interactions, one can derive a simpler form involving spherical Bessel functions rather than Coulomb wave functions. For the no-Coulomb example, one can show that $W = 0$ as $q \to 0$.

Using experimentally tabulated phase shifts [19], and the arbitrary choice of $\epsilon = 1$ fm, wave functions were numerically generated and convoluted with the source function through Eq. (1) to generate correlation functions. Correlations for pK^+ were only slightly affected by the strong interaction as can be seen in Fig.s 1 and 2. For this example, there are no resonant channels and the correlation is dominated by Coulomb.

Figure 3 shows results for $p\pi^+$ correlations which are dominated by the Δ^{++} resonance for Q_{inv} near the resonant momentum, $Q_{inv} = 450$ MeV. The correlation has a significant dip for $\cos\theta \sim \pm 1$. A flat correlation would have signaled an insensitivity to the shape of the source. The strong sensitivity stems from the $\cos\theta_{qr}$ dependence of $|\psi(\mathbf{q}, \mathbf{r})|^2$ which is then convoluted with the shape dependence in $g(\mathbf{v}, \mathbf{r})$ to provide shape information in $C(\mathbf{v}, \mathbf{q})$. The angular behavior of $|\psi(\mathbf{q}, \mathbf{r})|^2$ can be understood by viewing the partial wave expansion for a scattered wave. For large qr,

$$\psi(\mathbf{q}, \mathbf{r}) = e^{i\mathbf{q}\cdot\mathbf{r}} - \frac{e^{-iqr}}{2iqr}\sum_\ell(-1)^\ell P_\ell(\cos\theta_{qr})\left(e^{-2i\delta_\ell} - 1\right)$$
$$+ \mathcal{O}\,1/(qr)^2. \tag{22}$$

The angular sensitivity has two sources. Squaring the second term provides a contribution proportional to the square of the scattering amplitude, $|f(\Omega)|^2$. This contribution has the same angular behavior as a scattered plane wave. For the $p\pi$ example this would have led to maxima for $\cos\theta \sim \pm 1$ rather than the minima which are seen in Fig. 3. The second source of angular dependence stems from the interference between the initial plane wave and the partial wave corrections. This interference will be strongest in the direction $\cos\theta_{qr} = -1$ since the phases then share the same r dependence, e^{-iqr}. The source points in this direction are those from which the trajectories must pass directly over the origin. For $\cos\theta_{qr} = -1$, the wave function can be written as

$$\psi(\mathbf{q}, \mathbf{r})|_{\cos\theta_{qr}=-1}$$
$$= e^{-iqr}\left(1 + \sum_\ell(2\ell+1)e^{-i\delta_\ell}\sin\delta_\ell\frac{1}{2qr} + \mathcal{O}1/(qr)^2\right). \tag{23}$$

For small phase shifts $\cos\delta_\ell > 0$, and the interference is positive for attractive interactions (positive phase shifts) and is negative for repulsive interactions. This corresponds to the focusing or de-focusing effect of the potential in the direction of the interaction. For repulsive interactions this can be thought of as shadowing. At a resonance the phase shift is $\pi/2$ and there is no interference unless one includes higher order terms in the $(1/qr)$ expansion of the Hankel waves. For p waves this next term results in a negative interference which is responsible for the dip in the angular correlation shown in Fig. 3. In fact, when this calculation was repeated keeping only the lowest order term in the $1/(qr)$ expansion of the $\ell = 1$ partial wave, the dip at $\cos\theta = \pm 1$ in Fig. 3 disappeared.

Thus, the ability to determine the angular shape of a source through strong-interaction induced correlations is complex. Since the interference between the scattered partial wave and the initial plane wave in Eq. (23) is proportional to $\cos\delta\sin\delta$, one may wish to view the angular

correlation both above and below the resonance as $\cos\delta$ switches from positive to negative. Furthermore, an angular sensitivity might stem from higher order terms in the Hankel functions as was the case above. Understanding results with simple classical arguments can clearly be misleading, but fortunately, quantum calculations can be modeled in a straight-forward fashion if one has a good understanding of the phase shifts.

Strong and Coulomb induced correlations had been previously studied for their ability to unfold the angle-averaged source function, g, for both high-energy and low-energy collisions [20–22]. Our findings show that such correlations also have tremendous potential to discern shape characteristics and thus provide an estimate of source lifetimes. Determining shape and lifetime characteristics had been previously confined to analyses of identical-particle correlations. As strong and Coulomb correlations are of a manifestly different character than correlations from identical-particle interference, the analyses described here represent a truly independent strategy for determining space-time characteristics of hadronic sources.

[1] U. Heinz and B. Jacak, Ann. Rev. Nucl. Part. Sci. **49**, 529 (1999).
[2] S. Pratt, Phys. Rev. D **33**, 1314 (1986).
[3] M. Gyulassy and D. Rischke, Nucl. Phys. A **608**, 479 (1996).
[4] D. Teaney, J. Lauret, and E. Shuryak, nucl-th/0110037.
[5] S. Soff, S. Bass, and A. Dumitru, Phys. Rev. Lett. **86**, 3981 (2001).
[6] S. Pratt, T. Csörgő and J. Zimányi, Phys. Rev. C**42**, 2646 (1990).
[7] C. Adler et al. (STAR), Phys. Rev. Lett. **87**, 082301 (2001).
[8] K. Adcox et al. (PHENIX), Phys. Rev. Lett. **88**, 192302 (2002).
[9] M. Baker et al. (PHOBOS), nucl-ex/0212009.
[10] Y. Kim, R. de Souza, C. Gelbke, , W. Gong, and S. Pratt, Phys. Rev. C **45**, 387 (1992).
[11] R. Lednicky, V.L. Lyuboshitz B. Erazmus, and D. Nouais, Phys. Lett. B **373**, 20 (1996).
[12] C.J. Gelderloos et al., Phys. Rev. Lett. **75**, 3082 (1995).
[13] S. Voloshin, R. Lednicky, and S. Panitkin, Phys. Rev. Lett. **79**, 4766 (1997).
[14] D. Miskowiec, Proceedings of CRIS '98, World Scientific, 1998; www.arXiv.org/nucl-ex/9809003.
[15] R. Kotte et al., Eur. Phys. J. A **6**, 185 (1999); www.arXiv.org/nucl-ex/9904007.
[16] G. Baym and P. Braun-Munzinger, Nucl. Phys. A **610**, 286c (1996).
[17] B. Jennings, D. Boal, and J. Shillcock, Phys. Rev. C **33**,

1303 (1986).

[18] M. Abramowitz and I. Stegun, *Handbook of Mathematical Functions* (National Bureau of Standards, 1968), 7th ed.

[19] Nucleon-kaon and nucleon-pion phase shifts are available on-line from the Center for Nuclear Studies Data Analysis Center at George Washington University, http://gwdac.phys.gwu.edu/.

[20] D. A. Brown and P. Danielewicz, Phys. Rev. **C64**, 014902

(2001), nucl-th/0010108.

[21] S. Y. Panitkin et al. (E895), Phys. Rev. Lett. **87**, 112304 (2001), nucl-ex/0103011.

[22] G. Verde, P. Danielewicz, W. Lynch, D. Brown, C. Gelbke, and M. Tsang, Phys. Rev. **C65**, 054609 (2002), nucl-ex/0112004.